CRYSTAL GROWTH & DESIGN
2004
VOL. 4, NO. 1
63−70

Crystal Engineering of Luminescent Gold(I) Compounds of 2-Amino-5-mercapto-1,3,4-thiadiazolate and 6-Amino-2-mercaptobenzothiazolate

Biing-Chiau Tzeng,*,† Yung-Chi Huang,† Wan-Min Wu,† Shih-Yang Lee,† Gene-Hsiang Lee,‡ and Shie-Ming Peng‡

Department of Chemistry and Biochemistry, National Chung Cheng University, 160 San-Hsin, Min-Hsiung, Chia-Yi, Taiwan 621, and Department of Chemistry, National Taiwan University, Taipei, Taiwan

Received June 11, 2003; Revised Manuscript Received September 19, 2003

ABSTRACT: Treatment of monophosphine gold(I) complex [$P(CH_2CH_2CN)_3(AuCl)$] or bisphosphine gold(I) complex [$dpph(AuCl)_2$, dpph = 1,6-bis(diphenylphosphino)hexane] with sodium 2-amino-5-mercapto-1,3,4-thiadiazolate ($NaSSNH_2$) or sodium 6-amino-2-mercaptobenzothiazolate ($NaSSCNH_2$) affords a series of gold(I) thiolates: [$P(CH_2CH_2CN)_3(Au(SSNH_2))$] **1**, [$dpph(Au(SSNH_2))_2$] **2**, [$P(CH_2CH_2CN)_3(Au(SSCNH_2))$] **3**, and [$dpph(Au(SSCNH_2))_2$] **4**. The crystal structures of **1** and **1**·DMF feature a similar ribbon pattern with molecules linked through hydrogen-bonding interactions, and **2**·DMF displays a novel pseudo double-helical structure assembled into a two-dimensional sheet via hydrogen bonding. When the $SSNH_2$ ligand is replaced by $SSCNH_2$, the cyano group of the $P(CH_2CH_2CN)_3$ complex engaging in hydrogen-bonding interactions contributes to the formation of a two-dimensional sheet structure for **3**. Complex **4**, featuring a dinuclear S-shaped structure, is further associated into a one-dimensional chain via a weak N−H···S interaction. In the present work, the bulky $P(CH_2CH_2CN)_3$ ligands prevent gold(I)···gold(I) interactions in their complexes, but allow interesting hydrogen-bonding interactions. Somewhat unexpectedly, even complexes **2** and **4** bearing the more flexible dpph ligands do not display aurophilic interactions in the solid state. In addition, the frameworks studied herein all show photoluminescence upon incorporation of gold(I) centers, and potential applications in chemical sensing may be anticipated.

Introduction

Among gold(I) compounds, gold(I) thiolates are the most extensively used, with applications in medicine and surface technology. Virtually all of the classical and modern drugs based on gold(I) ions for arthritis and rheumatism have been gold(I)−sulfur compounds.[1−3] Following the theoretical prediction and experimental results of Pyykkö,[4] Balch[5] and their co-workers, it is anticipated that aurophilic interactions between the gold(I)−X units would be strengthened in the order of X = Cl < Br < I < thiolate in the absence of any steric effect. However, Laguna et al.[6] has recently concluded from experimental evidence and ab initio calculations on the gold(I)−imine system, that hydrogen bonding can compete against aurophilic interactions. Aurophilicity, the propensity for closed-shell d^{10} gold(I) centers to form weak bonding interactions, leading to the fabrication of supramolecular gold(I) compounds with novel structural and spectroscopic properties, has recently been an interesting phenomenon for study in gold chemistry.[7−16] In fact, it is well-known that aurophilicity is comparable in strength and energy with hydrogen bonding,[8a,b] and thus a delicate competition between these secondary interactions in the structural arrangement is anticipated when both can coexist in the solid state.

Most gold(I) thiolates show rich luminescence properties, and the emissions come mostly from the S → Au excitation, based on the pioneering work by Bruce and co-workers[17] on [Au(dppe)(pdt)Au] (515 nm; dppe = 1,2-bis(diphenylphosphino)ethane, pdt = 1,3-propanedithiolate) and [Au(dppb)(pdt)Au] (510 nm; dppb = 1,4-bis(diphenylphosphino)butane). The origin of the excited-state of gold(I) thiolates studied by Bruce and co-workers is not due to aurophilic interactions. This is quite different from the phosphine gold(I) compounds, whose luminescence properties have been well-documented and ascribed mostly to aurophilicity.[18] The correlation between the emission energy and the gold(I)···gold(I) interaction was studied by Fackler and co-workers[19] in a series of monomeric gold(I) complexes containing phosphine and aromatic thiolate ligands. However, no direct correlation has been found between the Au(I)···Au(I) distance and the emission energies. All of the compounds synthesized by Fackler et al luminesce at 77 K (485−702 nm) in the solid state, and the excitation was also assigned to a S → Au charge-transfer transition.

In a new approach to the broad area of applications of gold(I) thiolates, we have recently tried to exploit phenomena based on cooperative aurophilic and hydrogen-bonding interactions for crystal engineering. In earlier related studies,[20] we have chosen 2-amino-5-mercapto-1,3,4-thiadiazolate ($SSNH_2$) as a building block for the construction of interesting hydrogen-bonded frameworks with a novel combination of monophosphines (e.g., PPh_3 and PMe_3), bisphosphines (e.g., dppm [bis(diphenylphosphino)methane] and dppe [1,2-bis(diphenylphosphino)ethane]), and amino/thiolate ligands. In further work on this topic, we studied the crystal engineering and solid-state luminescence properties of complexes bearing the bulky $P(CH_2CH_2CN)_3$

* To whom correspondence should be addressed. E-mail: chebct@ccu.edu.tw.
† National Chung Cheng University.
‡ National Taiwan University.

10.1021/cg034097n CCC: $27.50
Published on Web 10/28/2003

Table 1. Crystallographic Data for 1, 1·DMF, 2·DMF, 3, and 4

	1	**1**·DMF	**2**·DMF	**3**	**4**
empirical formula	$C_{11}H_{14}AuN_6PS_2$	$C_{14}H_{21}AuN_7OPS_2$	$C_{37}H_{42}Au_2N_7OP_2S_4$	$C_{16}H_{17}AuN_5PS_2$	$C_{44}H_{42}Au_2N_4P_2S_4$
formula weight	522.34	595.43	1184.89	571.40	1210.93
crystal system	monoclinic	orthorhombic	triclinic	triclinic	triclinic
space group	$P2_1/c$	$Pna2_1$	$P\bar{1}$	$P\bar{1}$	$P\bar{1}$
a (Å)	8.7068(1)	8.9084(1)	11.5092(1)	9.0821(1)	9.1074(1)
b (Å)	20.1996(2)	27.0753(6)	14.4054(1)	11.5772(1)	9.7714(1)
c (Å)	8.9826(1)	8.6670(1)	14.5846(2)	18.3990(1)	12.9474(1)
α (°)			66.4609(4)	90.0484(3)	111.8273(5)
β (°)	92.7153(7)		71.2165(4)	90.6298(3)	95.6135(5)
γ(°)			84.2758(6)	91.2217(3)	96.9139(5)
V (Å^3)	1578.03(3)	2090.46(6)	2097.61(4)	1934.013(2)	1049.048(18)
ρ_{calc} (g cm^{-3})	2.199	1.892	1.876	1.962	1.917
Z	4	4	2	4	1
μ (Mo−Kα) (cm^{-1})	96.90	73.32	73.01	79.14	72.98
T (K)	150(1)	150(1)	150(1)	150(1)	150(1)
obsd reflns ($F_o \geq 2\sigma F_o$)	3629	4581	9608	8880	4834
refined parameters	191	236	479	452	254
R^a	0.0264	0.0370	0.0366	0.0303	0.0269
$R_w{}^b$	0.0595	0.0679	0.0856	0.0735	0.0633

^{a} $R = \sum||F_o| - |F_c||/\sum|F_o|$. ^{b} $wR_2=\{[\sum w(F_o^2 - F_c^2)^2/\sum[w(F_o^2)^2]\}^{1/2}$.

Scheme 1

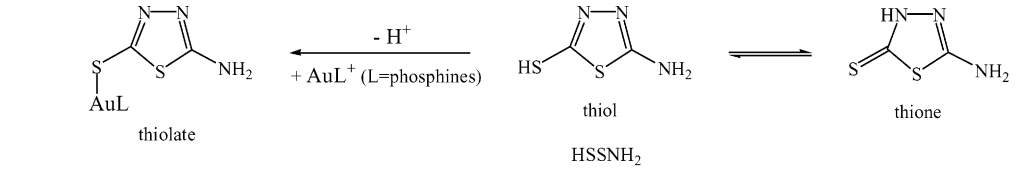

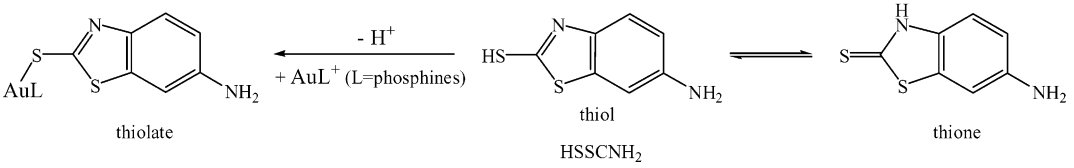

and the longer, more flexible dpph ligands, and $SSNH_2$ or $SSCNH_2$, since the steric demands or flexibility of the ligand backbones would be expected to strongly influence the structural properties and may help to elucidate the correlation between aurophilic interactions and hydrogen bonding in the formation of hydrogen-bonded frameworks.

Experimental Section

General Information. All reactions were performed under a nitrogen atmosphere. Solvents for syntheses (analytical grade) were used without further purification. NMR: Bruker DPX 400 MHz spectrometer; deuterated solvents were used with the usual standards. MS: Positive ion FAB mass spectra were recorded on a Finnigan MAT95 mass spectrometer. $HSSNH_2$ and $HSSCNH_2$ are commercially available, and $P(CH_2CH_2CN)_3(AuCl)$ and $dpph(AuCl)_2$ were prepared by literature methods.[21]

$[P(CH_2CH_2CN)_3(Au(SSNH_2))]$ 1. The reaction of $NaSSNH_2$ [155 mg, 1 mmol, obtained from $HSSNH_2$ (133 mg, 1 mmol) and NaOMe (57 mg, 1.05 mmol) in MeOH (25 mL)] with $P(CH_2CH_2CN)_3(AuCl)$ (426 mg, 1 mmol) in CH_2Cl_2/MeOH (1:1, 50 mL) at room temperature for 4 h gave a colorless solution. The solution was concentrated under vacuum to give a crystalline solid of $[Au(PPh_3)(SSNH_2)]$ in 60% yield. Single crystals of **1** were grown by slow evaporation of a CH_2Cl_2/MeOH solution and those of **1**·DMF grown by ether diffusion to a DMF solution. Since the solvates in **1**·DMF were easily lost from the crystal lattice, the crystals were instantly cracked in air. Consequently, further characterizations and spectroscopic measurements carried out on **1**·DMF were found to be similar to those of **1**. MS (FAB): $[P(CH_2CH_2CN)_3(Au(SSNH_2))]$, m/e = 523, 36%. {^{1}H} ^{31}P NMR (DMSO-d_6, 25 °C): δ 32.85 [s]. ^{1}H NMR ($CDCl_3$, 25°C): δ 2.50 [s, 6H, PCH_2], 2.86 [s, 6H, CH_2-CN], 6.71 [s, 2H, NH_2]. IR (KBr) υ_{NH2} 3280 and 3164, υ_{CH} (aliphatic) 2973, 2950 and 2913, $\upsilon_{C=N}$ 2251, $\upsilon_{C=N}$ 1604 and 1500 cm^{-1}. Anal. Calcd (%) for $C_{11}H_{14}AuN_6PS_2$: C, 25.27; H, 2.68; N, 16.08. Found (%): C, 25.59; H, 2.85; N, 16.31.

$[dpph(Au(SSNH_2))_2]$ 2. The reaction of $NaSSNH_2$ (155 mg, 1 mmol) with $dpph(AuCl)_2$ (460 mg, 0.5 mmol) in CH_2Cl_2/MeOH (1:1, 50 mL) at room temperature for 4 h gave a pale-yellow precipitate. The precipitate was isolated by vacuum filtration and pale-yellow solids of $[dppm(Au(SSNH_2))_2]$ were obtained in 62% yield. Single crystals of **2**·DMF were grown by ether diffusion to a DMF solution. MS (FAB): [dpph(Au-$(SSNH_2)$)Au], m/e = 980, 100%. {^{1}H} ^{31}P NMR (DMSO-d_6, 25 °C): δ 34.63 [s]. ^{1}H NMR (DMSO-d_6, 25 °C): δ 1.48 [s, 6H, $P(CH_2)_3$-], 6.74 [s, 2H, NH_2], 7.57−7.80 [m, 10H, PPh_2]. IR (KBr) υ_{NH2} 3121, υ_{CH} (aliphatic) 2924 and 2853, $\upsilon_{C=N}$ 1672 and 1515 cm^{-1}. Anal. Calcd (%) for $C_{34}H_{35}Au_2N_6P_2S_4$: C, 36.69; H, 3.15; N, 7.55. Found (%): C, 36.96; H, 2.95; N, 7.31.

$[P(CH_2CH_2CN)_3(Au(SSCNH_2))]$ 3. The reaction of $NaSSCNH_2$ [204 mg, 1 mmol, obtained from $HSSNH_2$ (182 mg, 1 mmol) and NaOMe (57 mg, 1.05 mmol) in MeOH (25 mL)] with $P(CH_2CH_2CN)_3(AuCl)$ (426 mg, 1 mmol) in CH_2Cl_2/MeOH (1:1, 50 mL) at room temperature for 4 h generated a pale-yellow precipitate. The precipitate was isolated by vacuum filtration and $[P(CH_2CH_2CN)_3(Au(SSCNH_2))]$ was obtained in 70% yield as a colorless solid. Single crystals of **3** were grown by ether diffusion to a DMF solution. MS (FAB): $[P(CH_2CH_2CN)_3(Au(SSCNH_2))]$, m/e = 572, 60%. {^{1}H} ^{31}P NMR (DMSO-d_6, 25 °C): δ 33.39 [s]. ^{1}H NMR (DMSO-d_6, 25 °C): δ 2.54 [m,

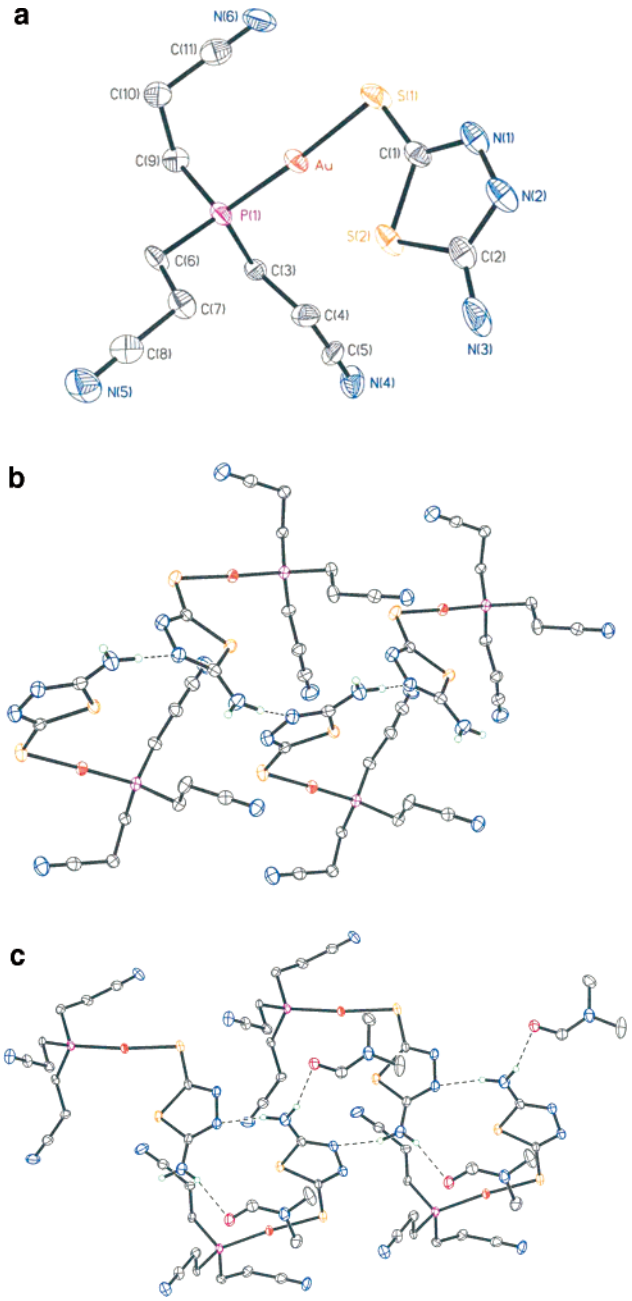

Figure 1. (a) Molecular structure of **1**. ORTEP diagram shows 50% probability ellipsoids. Selected bond lengths (Å) and angles (°) for **1**: Au−S(1) 2.3100(11), Au−P(1) 2.2565(11); P(1)−Au−S(1) 173.67(8) and for **1**·DMF: Au−S(1) 2.304(2), Au−P(1) 2.253(2); P(1)−Au−S(1) 175.07(9), (b) the hydrogen-bonded extended structure of **1**, and (c) the hydrogen-bonded extended structure of **1**·DMF.

6H, PCH_2], 2.92 [m, 6H, CH_2CN], 5.09 [s, 2H, NH_2], 6.58 [d, J_{HH} = 8.56 Hz, 1H, C(N)CH=C], 6.83 [s, 1H, C(=S)CH=C(N)], 7.28 [d, J_{HH} = 8.56 Hz, 1H, C=CHC(N)]. IR (KBr) υ_{NH2} 3324 and 3213, υ_{CH} (aliphatic) 2959 and 2921, $\upsilon_{C=N}$ 2247, $\upsilon_{C=N}$ 1600 and 1472 cm^{-1}. Anal. Calcd (%) for $C_{16}H_{17}AuN_5PS_2$: C, 33.60; H, 2.98; N, 12.25. Found (%): C, 33.72; H, 3.08; N, 12.18.

[dpph(Au(SSCNH$_2$))$_2$] 4. The reaction of $NaSSCNH_2$ (204 mg, 1 mmol) with $dpph(AuCl)_2$ (460 mg, 0.5 mmol) in CH_2Cl_2/MeOH (1:1, 50 mL) at room temperature for 4 h generated a pale yellow precipitate. The precipitate was isolated by filtration and [dpph(Au(SSCNH$_2$))$_2$] was obtained in 75% yield as a pale-yellow solid. Single crystals of **4** were grown by ether diffusion to a DMF solution. MS (FAB): [dpph(Au(SSCNH$_2$))-Au], *m/e* = 1030, 100%. {^{1}H} ^{31}P NMR (DMSO-d_6, 25 °C): δ 35.28 [s]. ^{1}H NMR (DMSO-d_6, 25 °C): δ 1.49 [s, 6H, $P(CH_2)_3$-],

Table 2. Hydrogen Bonds in the Structures of 1, 1·DMF, 2·DMF, 3, and 4[a]

complex	D−H···A (Å)	D−H (Å)	H···A (Å)	D···A (Å)	D−H···A (°)
1	N(3)−H(3B)···N(2′)	0.88	2.251	3.019	145.6
1·DMF	N(3)−H(3B)···N(2′)	0.88	2.062	2.891	156.6
	N(3)−H(3A)···O(1)	0.88	2.170	3.021	162.6
2·DMF	N(3)−H(3A)···N(5)[(a)]	0.88	2.167	2.972	155.7
	N(3)−H(3B)···N(4B)[(b)]	0.88	2.135	3.000	167.3
	N(6)−H(6A)···N(2)[(a)]	0.88	2.348	3.024	137.8
	N(6)−H(6B)···N(1B)[(b)]	0.88	2.172	3.019	161.4
3	N(2)−H(2B)···N(6)	0.88	2.235	3.104	169.4
	N(2)−H(2A)···N(9A)	0.88	2.251	3.130	176.7
	N(7)−H(7A)···N(1A)	0.88	2.189	3.068	177.3
	N(7)−H(7B)···N(4B)	0.88	2.238	3.105	168.0
4	N(2)−H(2A)···S(1)[(c)]	0.88	2.704	3.530	156.8

[a] Symmetry positions of atoms A: (a) $-x, -y+2, -z-2$; (b) $-x+1, -y+1, -z$; (c) $-x, -y+1, -z$.

Scheme 2

$AuCl(P(CH_2CH_2CN)_3) + NaX \longrightarrow [Au(P(CH_2CH_2CN)_3)X] + NaCl$

(X = $SSNH_2$ **1**, $SSCNH_2$ **3**)

$dpph(AuCl)_2 + 2\,NaX \longrightarrow [dpph(AuX)_2] + 2\,NaCl$

(X = $SSNH_2$ **2**, $SSCNH_2$ **4**)

5.09 [s, 2H, NH_2], 6.62 [d, J_{HH} = 8.6 Hz, 1H, C(N)CH=C], 6.83 [s, 1H, C(=S)CH=C(N)], 7.32 [d, J_{HH} = 8.56 Hz, 1H, C=CHC-(N)], 7.55−7.83 [m, 10H, PPh_2]. IR (KBr) υ_{NH2} 3335 and 3202, υ_{CH} (aliphatic) 2921 and 2850, $\upsilon_{C=N}$ 1617 and 1469 cm^{-1}. Anal. Calcd (%) for $C_{44}H_{42}Au_2N_4P_2S_4$: C, 43.60; H, 3.47; N, 4.62. Found (%): C, 43.41; H, 3.35; N, 4.61.

Physical Measurements and Instrumentation. Steady-state emission spectra were obtained on a SPEX Fluorolog-2 spectrophotometer, and emission lifetime measurements were performed with a Quanta Ray DCR-3 Nd:YAG laser (pulse output 355 nm, 8 ns). The decay signal was recorded by a R928 PMT (Hamamatsu), connected to a Tektronix 2430 digital oscilloscope.

X-ray Crystallography. Suitable crystals were mounted on glass capillaries. Data collection was carried out on a Bruker SMART CCD diffractometer with Mo radiation at 150 K. Preliminary orientation matrices and unit cell parameters were determined from three runs of 15 frames each, each frame corresponding to 0.3° scan in 15 s, followed by spot integration and least-squares refinements. Data were measured using an ω scan of 0.3° per frame for 20 s until a complete hemisphere had been collected. Cell parameters were retrieved using SMART[22] software and refined with SAINT[23] on all observed reflections. Data reductions were performed with the SAINT software and corrected for Lorentz and polarization effects. Absorption corrections were applied with the program SADABS.[24] The structures were solved by direct methods with the SHELX93[25] program and refined by full-matrix least-squares methods on F^2 with SHEXLTL-PC V 5.03.[25] All non-hydrogen atomic positions were located in difference Fourier maps and refined anisotropically. The hydrogen atoms were placed in their geometrically generated positions. Detailed data collection and refinement of the complexes are summarized in Table 1, and their hydrogen bonds in the structures given in Table 2.

Results and Discussion

The crystal structure of $HSSNH_2$ is a supramolecular aggregate having S···S, S···N, N···N, and weak N−H ···S hydrogen-bonding.[26] The bond distances indicate that this compound exists in the thione rather than in the thiol form (Scheme 1).[5] As a new approach to molecular solids through the formation of complementary hydrogen-bonding interactions, preorganized dimer-

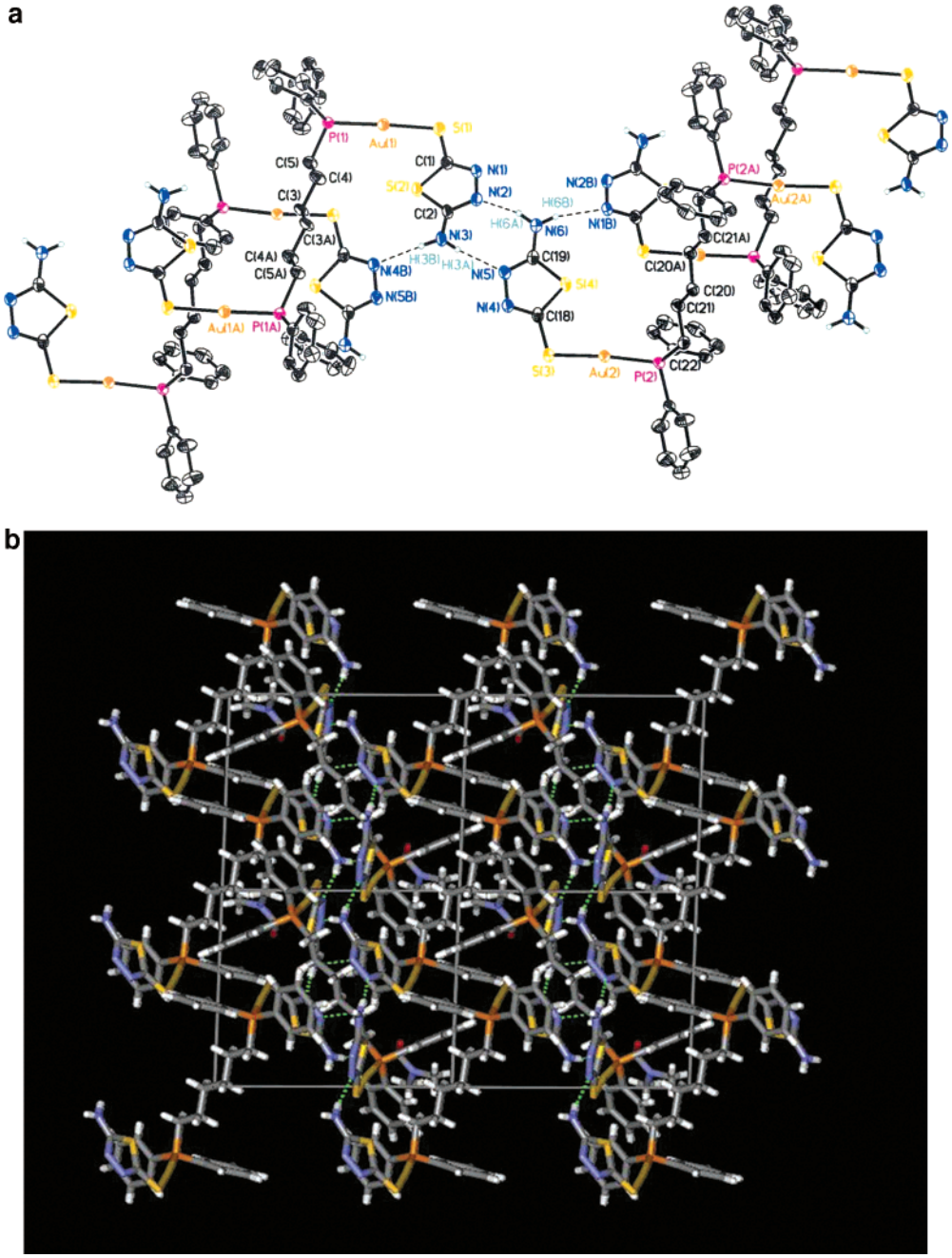

Figure 2. (a) Part of the hydrogen-bonded framework of **2** shows a novel double-helical structure and ORTEP diagram shows 50% probability ellipsoids. Selected bond lengths (Å) and angles (°): Au(1)−S(1) 2.3095(14), Au(2)−S(3) 2.3082(14), Au(1)−P(1) 2.2589(14), Au(2)−P(2) 2.2637(14); P(1)−Au(1)−S(1) 177.06(5), P(2)−Au(2)−S(3) 172.41(5), and (b) its two-dimensional hydrogen-bonded extended structure.

ic $[SSNH_2]_2$ moieties of the PPh_3 gold(I) complex have been further assembled into a ladder structure.[20] By reducing the steric effect of the phosphine units from PPh_3 to PMe_3, novel two-dimensional sheet frameworks have been built via cooperative intermolecular aurophilic and hydrogen-bonding interactions in the solid state.[20] That these dimeric $[SSNH_2]_2$ moieties are preorganized into one-dimensional ladder or two-dimensional sheets holds promise in the use of these ligands in the formation of new functional molecular solids. Thus, different structural motifs are anticipated for the $P(CH_2CH_2CN)_3$ and dpph gold(I) complexes of $SSNH_2$, because of the change in the bulkiness and/or flexibility of $P(CH_2CH_2CN)_3$, as well as the possible involvement of the CN group in hydrogen bonding with $SSNH_2$. There are no precedented studies in the literature about the behavior of the $SSCNH_2$ ligand with hydrogen-bonding functional groups as that in $SSNH_2$ (Scheme 1). The phosphine gold(I) thiolates studied herein were obtained in good to moderate yields (60−75%) and characterized by elemental analysis, FAB mass spectrometry, NMR and IR spectroscopy (Experimental Section), and they all show low-energy emissions. The preparation of these compounds is shown in Scheme 2.

It should be mentioned that, although the cone angle of $P(CH_2CH_2CN)_3$ (132°) is smaller than that of PPh_3 (145°),[27] some structural features cause $P(CH_2CH_2CN)_3$ to be sterically more demanding than one would have

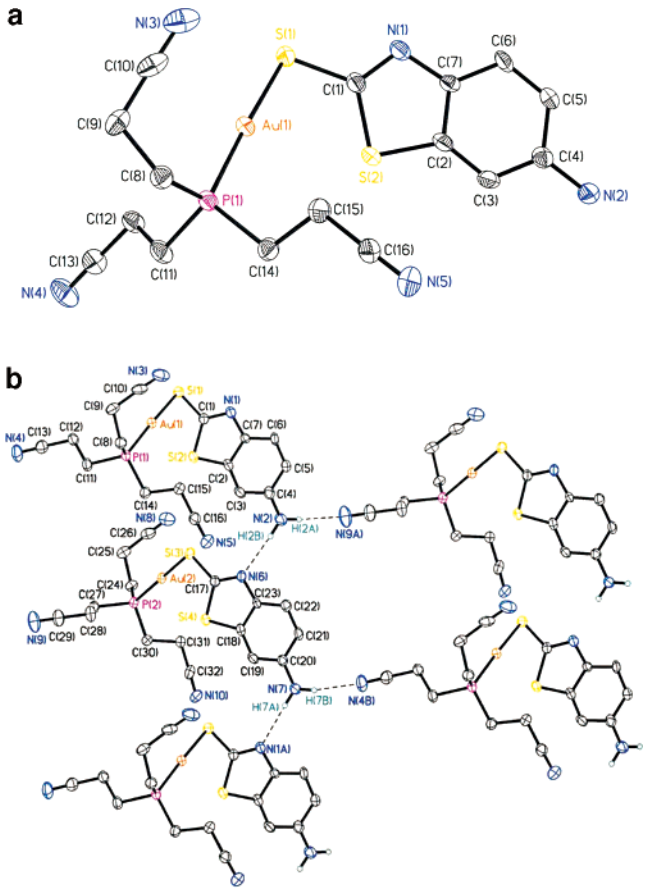

Figure 3. (a) Molecular structure of **3**. ORTEP diagram shows 50% probability ellipsoids. Selected bond lengths (Å) and angles (°): Au(1)−S(1) 2.3086(11), Au(2)−S(3) 2.3087(12), Au(1)−P(1) 2.2564(11), Au(2)−P(2) 2.2576(12); P(1)−Au-S(1) 177.45(4), P(2)−Au(2)-S(3) 178.94(4), and (b) its hydrogen-bonded extended structure.

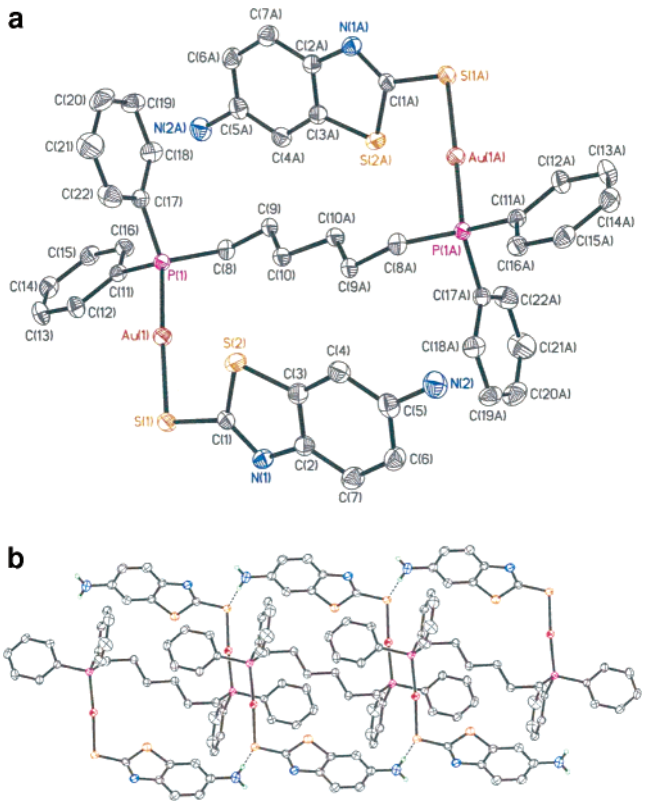

Figure 4. (a) Molecular structureof **4**. ORTEP diagram shows 50% probability ellipsoids. Selected bond lengths (Å) and angles (°): Au(1)−S(1) 2.3190(11), Au(1)−P(1) 2.2649(11); P(1)−Au(1)−S(1) 171.13(4), and (b) its hydrogen-bonded extended structure.

expected based solely on the cone angle. $P(CH_2CH_2CN)_3$ adopted an inverted umbrella conformation in $[(P(CH_2CH_2CN)_3)_2Au]Cl$ or *trans*-$[PtCl_2(P(CH_2CH_2CN)_3)_2]$ as reported by Fackler et al.[28] This was also the case for the complexes studied in this work. Unlike $[(PPh_3)_2AuCl]$, which is three-coordinate with a P−Au−P angle of 132°, the chloride in $[(P(CH_2CH_2CN)_3)_2Au]Cl$ is not coordinated to gold as that in $[(P(cyclohexyl)_3)_2Au]Cl$.[29] The encapsulation of the gold is also observed in $[(P(CH_2CH_2CN)_3)_2Au]Cl$, and the Au(I)···N≡C interaction (3.58 Å; the sum of van de Waals radii, 3.25 Å) is suggested to be responsible for the inverted umbrella conformation of $P(CH_2CH_2CN)_3$ according to the MM2 results of CAChe molecular modeling.[28] Thus, $P(CH_2CH_2CN)_3$ is at least as bulky as PPh_3, even though the former has a smaller cone angle.

Description of Crystal Structure. Perspective views of **1**, **1**·DMF, **2**·DMF, **3**, and **4** and their extended structures are shown in Figures 1−4, respectively. The gold(I) centers are all two-coordinate and adopt an almost linear geometry with P−Au−S angles ranging from 171.13(4) to 178.94(4)°. The Au−P [2.253(2)−2.2649(11)Å] and Au−S [2.304(2)−2.3190(11) Å] distances fall in the normal range.[20] On the basis of the observed bonding parameters, $SSNH_2$ and SSCNH are in the thiolate rather than in the thione form, and this is also supported by the C−S distances, which are within 1.745(5)−1.750(4) Å and are typical of coordinated thiolates.[30]

As shown in Figure 1, any close gold(I)···gold(I) contact seems to have been prevented by the bulky $P(CH_2CH_2CN)_3$ ligands for both **1** and **1**·DMF. However, the crystal structures of **1** and **1**·DMF feature a similar ribbon pattern, with molecules associated through hydrogen-bonding interactions [N(3)−H(3A)···N(2′), N(3)···N(2′) 3.019 Å] and [N(3)−H(3A)···N(2′), N(3)···N(2′) 2.891 Å], respectively. The $SSNH_2$ ligands are engaged in head-to-tail hydrogen-bonding interactions. One of the two N−H moieties of each -NH_2 group is engaged in hydrogen bonding to one DMF molecule [N(3)−H(3B)···O(1), N(3)···O(1) 3.021 Å] in **1**·DMF. Interestingly, removing the DMF molecule from **1**·DMF seems to lead to the formation of **1** with shrinking in only one dimension. The structural motifs of **1** and **1**·DMF are different from the ladder structures or dimeric forms of the PPh_3 complexes of $SSNH_2$, with or without solvates.[20] The present structures thus represent a totally new type of hydrogen bonding for $SSNH_2$.

Intra- and intermolecular Au(I)···N≡C interactions with distances of 3.63 and 3.71 Å, respectively, are found in **1**, but in **1**·DMF, only an intramolecular Au(I)···N≡C interaction with a distance of 3.38 Å was observed. Again, these weak Au(I)···N≡C interactions are said to be responsible for the inverted umbrella conformation of $P(CH_2CH_2CN)_3$. In the present work, the bulky $P(CH_2CH_2CN)_3$ gold(I) complexes inhibit gold(I)···gold(I) interactions, but facilitated interesting hydrogen-bonding interactions.

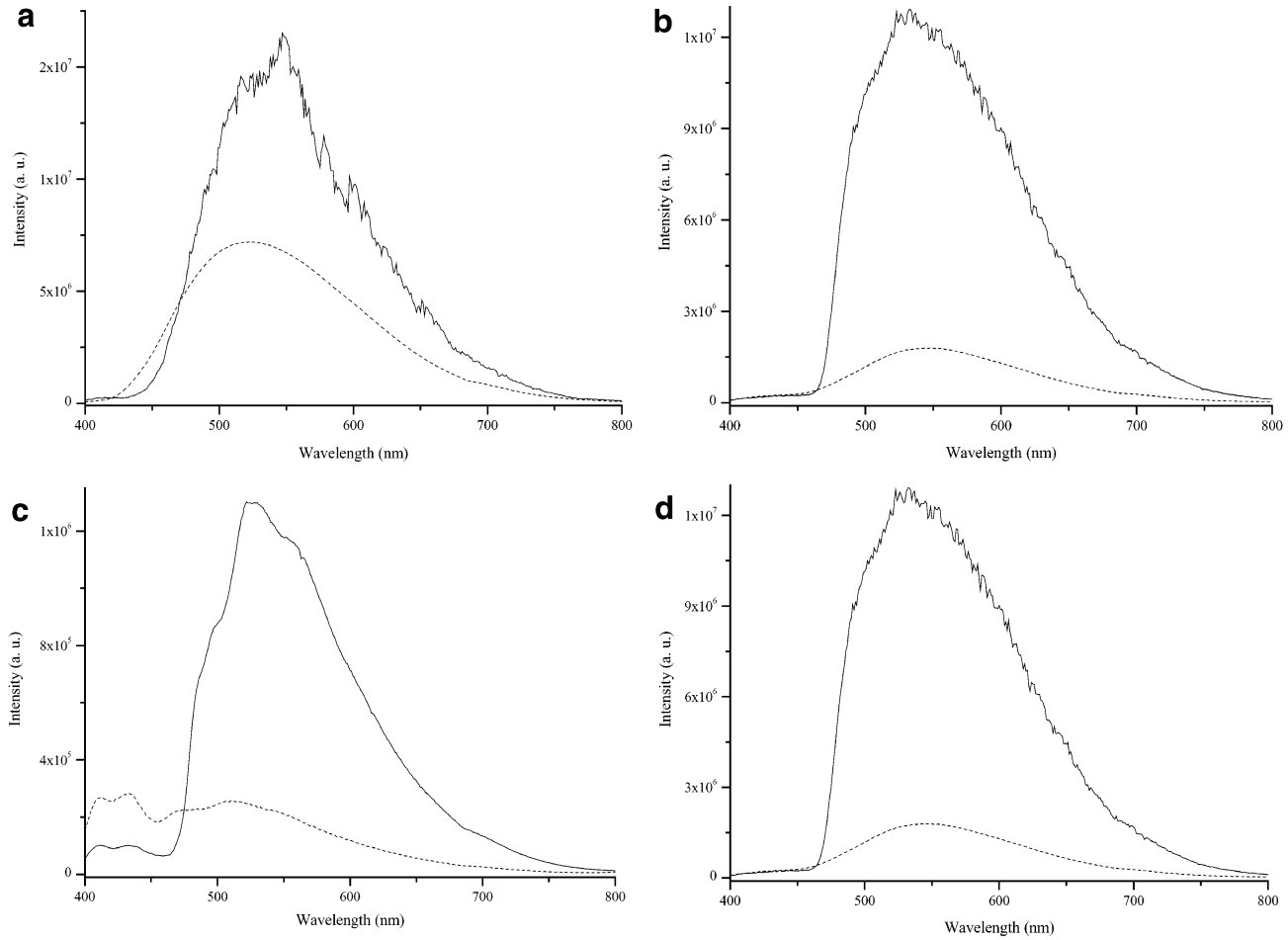

Figure 5. Emission spectra of **1** (a), **2** (b), **3** (c), and **4** (d) measured in the solid state at 298 K (dash) and at 77 K (solid), respectively. Excitation at 355 nm.

Each asymmetric unit of the dpph gold(I) complex **2** contains one DMF molecule, but there are no hydrogen bonding interactions between the DMF and $SSNH_2$ moieties. Part of the hydrogen-bonded framework, showing a novel double-helical structure and its extended two-dimensional sheet, are shown in Figure 2 panels a and b, respectively. The structure can first be described as a ribbon pattern generated by head-to-tail, bifurcated hydrogen bonds of the $SSNH_2$ moieties [N(3)−H(3A)···N(5), N(3)···N(5) 2.972 Å; N(6)−H(6A)···N(2), N(6)···N(2) 3.024 Å]. The other N−H moiety of each -NH_2 group is involved in hydrogen bonding to $SSNH_2$, leading to a novel pseudo double-helical structure which is further assembled into a two-dimensional sheet [N(6)−H(6B)···N(1B), N(6)···N(1B) 3.019 Å; N(3)−H(3B)···N(4B), N(3)···N(4B) 3.000 Å]. Any close gold(I)···gold(I) contact is still absent in this structure; this was originally unexpected because of the greater flexibility of dpph over dppe was anticipated to facilitate aurophilic interactions. In a previous study,[20] the dppm gold(I) complex featured dinuclear units associated into a meandering chain structure via intramolecular aurophilic interactions at distances of 3.0987(10) Å and intermolecular hydrogen-bonds. The dppe gold(I) complex formed a complicated network via cooperative intermolecular aurophilic interactions at distances of 3.0987(10) Å and hydrogen bonding. Dppe is more flexible than dppm, and thus it was more likely that its related complex would have aurophilic interactions in the solid state. When it was found that the dpph gold(I) complex, whose dpph ligand was even more flexible than dppe, did not show any aurophilic interactions in the solid state, it was somewhat unexpected, since Pyykkö,[4] Balch[5] and their co-workers proposed that aurophilic interactions between the gold(I)−X units would be strengthened in the order of X = Cl < Br < I < thiolate in the absence of any steric effect.

The molecular structure and the hydrogen-bonded extended structure of complex **3** are shown in Figure 3 panels a and b, respectively. Complex **3** features a one-dimensional chain generated by slipped head-to-tail hydrogen bonds of the $SSCNH_2$ moieties [N(2)−H(2B)···N(6), N(2)···N(6) 3.104 Å; N(7)−H(7A)···N(1A), N(7)···N(1A) 3.068 Å]. Surprisingly, unlike those in **1** and **1**·DMF, one of the three cyano groups of $P(CH_2CH_2CN)_3$ is engaged in hydrogen bonding [N(2)−H(2A)···N(9A), N(2)···N(9A) 3.130 Å; N(7)−H(7B)···N(4B), N(7)···N(4B) 3.105 Å] and because of this additional interaction, the chain is further assembled into a two-dimensional sheet structure. The incorporation of $SSCNH_2$, instead of $SSNH_2$, allowed the cyano group of the $P(CH_2CH_2CN)_3$ gold(I) complex to also engage in hydrogen bonding and hence increases the complexity of the overall framework. The other two cyano groups remain uninvolved, and this is most likely due to steric constraints or crystal packing. Again, there are intra- and intermolecular Au(I)···N≡C interactions in **3**, of 3.44 and 3.52 Å, respectively.

Table 3. Solid-State Luminescence Data and Lifetimes of 1, 2, 3, and 4[a]

complex	emission max, nm	lifetime, μs
1	523 (298 K)	0.45
	548 (77 K)	810.00
2	412, 433	0.30
	560 (298K)	0.81
	410, 435	0.35
	533 (77K)	122.44
3	412, 434	0.37
	508, 545, 590 (298 K)	0.33
	414, 435	0.35
	522, 560 (77 K)	15.60
4	548 (298 K)	6.08
	533 (77 K)	345.81

[a] Excitation at 355 nm.

The molecular structure and the one-dimensional hydrogen-bonded structure of complex **4** are shown in Figure 4 a and b, respectively. Complex **4** features a dinuclear S-shape aggregate, with an inversion center at the midpoint of C(10)−C(10A). The S-shaped structure is associated into a chain structure through weak N(2)−H(2A)···S(1) (N(2)···S(1) 3.530 Å) interactions. The dpph is in an anti-conformation as in complex **2**, and the dramatic structural differences between complexes **2** and **4** seem only to be due to the variation in structural moieties of $SSNH_2$ and $SSCNH_2$.

Solid-State Emission Spectra. The phosphine gold(I) thiolates studied in this work all show solid-state luminescence at room temperature and at 77 K, as shown in Figure 5. The luminescence data and lifetimes in the solid state are summarized in Table 3. At room temperature, complexes **1**, **2**, and **4** show emissions at 523−560 nm upon photoexcitation at 355 nm. Upon cooling to 77 K, their solid-state emissions increase in intensity, but without any notable shift in energy (533−548 nm) or vibronic structures. However, the emission of complex **3** displays poor vibronic structure with peak maxima at ca. 508, 545, and 590 nm at room temperature, and a dramatic increase in emission intensity with peak maxima at ca. 522 and 560 nm upon cooling to 77 K. This progression, with a spacing at 1300−1400 cm^{-1}, is mostly due to the C═C or C═N stretching mode of the $SSCNH_2$ ligand. According to Bruce's[17] and Fackler's[19] studies, the emissive excited state is tentatively assigned to a S → Au charge-transfer transition. The complexes studied herein did not show any aurophilic interactions, so the S → Au charge-transfer excitation could not be modified by any gold(I)···gold(I) interactions. There are additional high-energy emissions at 410−435 nm for complexes **2** and **3**, and both are quite similar and thus expected to have similar emission origins. Because $P(CH_2CH_2CN)_3$ and PPh_3 show solid-state emission energies at 408 and 447 nm, respectively, the aforementioned high-energy emissions are unlikely to be related to the phosphine ligands. On the other hand, $HSSNH_2$ and $HSSCNH_2$ show solid-state emission energies at 410 and 426 nm, respectively, which are quite comparable to the high-energy emissions of complexes **2** and **3** at 410−435 nm. Thus, these high-energy emissions are most likely due to an intraligand transition of $SSNH_2$ or $SSCNH_2$. However, scattering from the solid samples contributes to these emissions cannot be excluded upon photoexcitation at 300−400 nm.

It was noted in Fackler's study that the emission energy can be tuned either by changing the substituents of the thiolates or by gold(I)···gold(I) interactions in the solid state.[19] The substituents on the thiolates exert direct effects on the S → Au charge-transfer transition energy, whereas the substituents on the phosphines have only indirect effects. ^{31}P NMR showed that the chemical shifts of $[Au(PMe_3)(SSNH_2)]$, $[AuP(CH_2CH_2CN)_3(SSNH_2)]$, $[dpph(AuSSNH_2)_2]$, and $[Au(PPh_3)(SSNH_2)]$ are −1.54, 32.85, 34.63, and 37.02, ppm respectively; thus, the electron-donating strengths of $P(CH_2CH_2CN)_3$ and dpph are comparable. We also measured the solid-state emission of $[Au(PPh_3)(SSNH_2)]$ to have a maximum at 524 nm; thus, the dependence of emission energies on the electron-donating strength of phosphines is not really obvious. Actually, the triplet-state (spin-forbidden) transition cannot be accounted for in a straightforward manner, and the factors responsible for these emission energies are much more complicated.

Conclusion

To construct functional materials that utilize hydrogen-bonding interactions as weak intermolecular forces facilitating self-assembly of the components is a current interest and synthetic challenge. In this work, we have prepared and characterized a series of phosphine gold(I) thiolates of $SSNH_2$ or $SSCNH_2$, leading to the formation of interesting hydrogen-bonded frameworks. By using the bulky $P(CH_2CH_2CN)_3$ or the longer and more flexible dpph as ligands, along with $SSNH_2$, the new gold(I) complexes show different macroscopic structures, unlike those of the related PPh_3 and dppe gold(I) complexes.[20] The crystal structures of **1** and **1**·DMF feature similar ribbon patterns with molecules associated through intermolecular hydrogen-bonding interactions. **2**·DMF shows a novel pseudo double-helical structure associated into a two-dimensional sheet via hydrogen bonding, and there is no evidence of close gold(I)···gold(I) contact. With $SSNH_2$ replaced by $SSCNH_2$, the cyano group of $P(CH_2CH_2CN)_3$ engages in hydrogen-bonding and contributes to the formation of a two-dimensional sheet structure of **3**. Complex **4**, featuring a dinuclear S-shaped structure, is further associated into a one-dimensional chain via weak N−H···S interactions. In the present study, the changing of the structural backbone of the auxiliary ligands or the substituents of the thiolates represents a totally different approach for designing and constructing new hydrogen-bonded materials. The strategy in this study has been successful in crystal engineering, and with the luminescence afforded by gold(I) centers, the luminescent solid-state materials studied herein are anticipated to find future applications in chemical sensing.

Acknowledgment. We thank the National Science Council and National Chung Cheng University of the Republic of China for financial support (NSC 90-2113-M-194-028 and 91-2113-M-194-019).

References

(1) (a) Shaw, C. F., III; Coffer, M. T.; Klingbeil, J.; Mirabelli, C. K. *J. Am. Chem. Soc.* **1988**, *110*, 729. (b) Coffer, M. T.; Shaw, C. F., III; Eidsness, M. K.; Watkins, J. W., II; Elder, R. C. *Inorg. Chem.* **1986**, *25*, 333. (c) Isab, A. A.; Sadler, P. J. *J. Chem. Soc., Dalton Trans.* **1982**, 135.

(2) Rapson, W. S. *Gold Usage*; Academic Press: London, 1978.
(3) Bain, C. D.; Whitesides, G. M. *Angew. Chem., Int. Ed. Engl.* **1989**, *28*, 506.
(4) Pyykkö, P.; Li, J.; Runeberg, N. *Chem. Phys. Lett.* **1994**, *218*, 133.
(5) Calcar, P. M. V.; Olmstead, M. M.; Balch, A. L. *Chem. Commun.* **1996**, 2597.
(6) Codina, A.; Fernández, E. J.; Jones, P. G.; Laguna, A.; López-de-Luzuriaga, J. M.; Monge, M.; Olmos, M. E.; Pérez, J.; Rodríguez, M. A. *J. Am. Chem. Soc.* **2002**, *124*, 6781.
(7) (a) Pyykkö, P. *Chem. Rev.* **1997**, *97*, 597. (b) Pyykkö, P.; Zhao, Y. *Angew. Chem., Int. Ed. Engl.* **1995**, *34*, 1894. (c) Pyykkö, P.; Li, J.; Runeberg, N. *Chem. Phys. Lett.* **1994**, *218*, 133. (d) Pyykkö, P.; Zhao, Y. *Chem. Phys. Lett.* **1991**, *177* 103. (e) Rösch, N.; Görling, A.; Ellis, D. E.; Schmidbaur, H. *Angew. Chem., Int. Ed. Engl.* **1989**, *28*, 1357. (f) Burdett, J. K.; Eisenstein, O.; Schweizer, W. B. *Inorg. Chem.* **1994**, *33*, 3261.
(8) (a) Schmidbaur, H. *Gold Bull.* **1990**, *23*, 11. (b) Schmidbaur, H.; Scherbaum, F.; Huber, B.; Müller, G. *Angew. Chem., Int. Ed. Engl.* **1988**, *27*, 419. 2. (c) Schmidbaur, H. *Chem. Soc. Rev.* **1995**, *24*, 391. (d) Schmidbaur, H. *Interdiscip. Sci. Rev.* **1992**, *17*, 213. (e) Schmidbaur, H. *Gold Bull.* **2000**, *33*, 1. (f) *Gold-Progress in Chemistry, Biochemistry and Technology*; Schmidbaur, H., Ed.; John Wiley & Sons: Chichester, U.K., 1999.
(9) (a) Vickery, J. C.; Olmstead, M. M.; Fung, E. Y.; Balch, A. L. *Angew. Chem., Int. Ed. Engl.* **1997**, *36*, 1179. (b) Vickery, J. C.; Balch, A. L. *Inorg. Chem.* **1997**, *36*, 5978. (c) Calcar, P. M. V.; Olmstead, M. M.; Balch, A. L. *Inorg. Chem.* **1997**, *36*, 5231. (d) Calcar, P. M. V.; Olmstead, M. M.; Balch, A. L. *J. Chem. Soc., Chem. Commun.* **1995**, 1773.
(10) (a) Fackler, J. P., Jr. *Polyhedron* **1997**, *16*, 1. (b) Fackler, J. P., Jr. *Inorg. Chem.* **2002**, *41*, 6959.
(11) (a) Puddephatt, R. J. *Coord. Chem. Rev.* **2001**, *216*−*217*, 313. (b) Puddephatt, R. J. *Chem. Commun.* **1998**, 1055. (c) Puddephatt, R. J. *The Chemistry of Gold*; Elsevier: Amsterdam, 1978.
(12) (a) Contel, M.; Garrido, J.; Gimeno, M. C.; Jones, P. G.; Laguna, A.; Laguna, M. *Organometallics* **1996**, *15*, 4939. (b) Gimeno, M. C.; Laguna, A. *Chem. Rev.* **1997**, *97*, 511.
(13) (a) Mingos, D. M. P.; Yau, J.; Menzer, S.; Williams, D. J. *Angew. Chem., Int. Ed. Engl.* **1995**, *34*, 1894. (b) Mingos, D. M. P. *J. Chem. Soc., Dalton Trans.* **1996**, 561.
(14) (a) Jones, P. G.; Ahrens, B. *New J. Chem.* **1998**, 104. (b) *Chem. Ber./Recueil* **1997**, *130*, 1813. (c) Vicente, J.; Chicote, M.-T.; Abrisqueta, M.-D.; Guerrero, R.; Jones, P. G. *Angew. Chem., Int. Ed. Engl.* **1997**, *36*, 1203.
(15) (a) Yam, V. W.-W.; Lo, K. K.-W. *Chem. Soc. Rev.* **1999**, *28*, 323. (b) Yam, V. W.-W.; Cheng, E. C.-C. *Angew. Chem., Int. Ed.* **2000**, *39*, 4240. (c) Yam, V. W.-W.; Cheng, E. C.-C. *Gold Bull.* **2001**, *34*, 20.
(16) (a) Tzeng, B.-C.; Lo, W.-C.; Che, C.-M.; Peng, S.-M. *Chem. Commun.* **1996**, 181. (b) Tzeng, B.-C.; Cheung, K.-K.; Che, C.-M. *Chem. Commun.* **1996**, 1681. (c) Tzeng, B.-C.; Che, C.-M.; Peng, S.-M. *J. Chem. Soc., Dalton Trans.* **1996**, 1769. (d) Tzeng, B.-C.; Chan, C.-K.; Cheung, K.-K.; Che, C.-M.; Peng, S.-M. *Chem. Commun.* **1997**, 135. (e) Tzeng, B.-C.; Che, C.-M.; Peng, S.-M. *Chem. Commun.* **1997**, 1771.
(17) (a) Che, C.-M.; Kwong, H.-L.; Yam, V. W.-W.; Cho, K.-C. *J. Chem. Soc., Chem. Comm.* **1989**, 885. (b) King, C.; Wang, J.-C.; Khan, M. N. I.; Fackler, J. P., Jr. *Inorg. Chem.* **1989**, *28*, 2145. (c) Gade, L. H. *Angew. Chem., Int. Ed. Engl.* **1997**, *36*, 1171. (d) Fu, W.-F.; Chan, K.-C.; Miskowski, V. M.; Che, C.-M. *Angew. Chem., Int. Ed.* **1999**, *38*, 2783.
(18) (a) Narayanaswamy, R.; Young, M. A.; Parkhurst, E.; Ouellette, M.; Kerr, M. E.; Ho, D. M.; Elder, R. C.; Bruce, A. E.; Bruce, M. R. M. *Inorg. Chem.* **1993**, *32*, 2506. (b) Jones, W. B.; Yuan, J.; Narayanaswamy, R.; Young, M. A.; Elder, R. C.; Bruce, A. E.; Bruce, M. R. M. *Inorg. Chem.* **1995**, *34*, 1996.
(19) Forward, J. M.; Bohmann, D.; Fackler, J. P., Jr.; Staples, R. J. *Inorg. Chem.* **1995**, *34*, 6330.
(20) Tzeng, B.-C.; Schier, A.; Schmidbaur, H. *Inorg. Chem.* **1999**, *38*, 3978.
(21) (a) Schmidbaur, H.; Wohlleben, A.; Wagner, F.; Orama, O.; Huttner, G. *Chem. Ber.* **1977**, *110*, 1748. (b) Eggleston, D. S.; McArdle, J. V.; Zuber, G. E. *J. Chem. Soc., Dalton Trans.* **1987**, 677.
(22) *SMART V 4.043 Software for the CCD Detector System*; Siemens Analytical Instruments Division: Madison, WI, 1995.
(23) *SAINT V 4.035 Software for the CCD Detector System*; Siemens Analytical Instruments Division: Madison, WI, 1995.
(24) Sheldrick, G. M. SHELXL-93, Program for the Refinement of Crystal Structures, University of Gottingen, Gottingen, Germany, 1993.
(25) SHELXTL 5.03 (PC−Version), Program Library for Structure Solution and Molecular Graphics, Siemens Analytical Instruments Division: Madison, WI, 1995.
(26) Downie, T. C.; Harrison, W.; Raper, E. S. *Acta Crystallogr.* **1972**, *B28*, 1584.
(27) Pruchnik, F. P.; Smoleński, P.; Wajda-Hermanowicz, K. *J. Organomet. Chem.* **1998**, *570*, 63.
(28) Khan, M. N. I.; King, C.; Fackler, J. P., Jr.; Winpenny, R. E. P. *Inorg. Chem.* **1993**, *32*, 2502.
(29) Muir, J. A.; Muir, M. M.; Pulsar, L. B.; Jones, P. G.; Sheldrick, G. M. *Acta Crystallogr.* **1985**, *C41*, 1174.
(30) Umakoshi, K.; Ichimura, A.; Kinoshita, I.; Ooi, S. *Inorg. Chem.* **1990**, *29*, 4005.

CG034097N